

UCRL-JC-124879

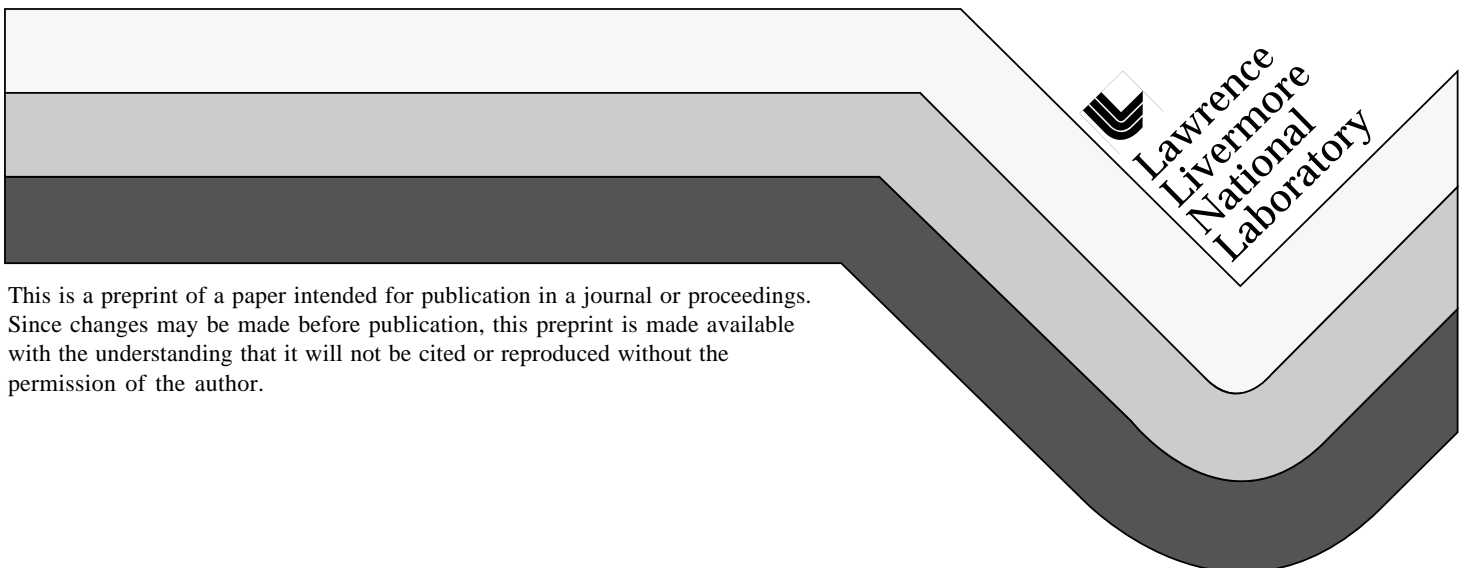
PREPRINT

**Morphologies of Laser-Induced Damage  
in Hafnia-Silica Multilayer Mirror and Polarizer Coatings**

F. Y. Génin  
C. J. Stolz

This paper was prepared for submittal to the  
Third International Workshop on Laser Beam and Optic Characterization  
Quebec, Canada  
July 8-10, 1996

**August 22, 1996**



This is a preprint of a paper intended for publication in a journal or proceedings.  
Since changes may be made before publication, this preprint is made available  
with the understanding that it will not be cited or reproduced without the  
permission of the author.

#### DISCLAIMER

This document was prepared as an account of work sponsored by an agency of the United States Government. Neither the United States Government nor the University of California nor any of their employees, makes any warranty, express or implied, or assumes any legal liability or responsibility for the accuracy, completeness, or usefulness of any information, apparatus, product, or process disclosed, or represents that its use would not infringe privately owned rights. Reference herein to any specific commercial product, process, or service by trade name, trademark, manufacturer, or otherwise, does not necessarily constitute or imply its endorsement, recommendation, or favoring by the United States Government or the University of California. The views and opinions of authors expressed herein do not necessarily state or reflect those of the United States Government or the University of California, and shall not be used for advertising or product endorsement purposes.

## Morphologies of laser-induced damage in hafnia-silica multilayer mirror and polarizer coatings

3<sup>rd</sup> Int. Workshop on Laser Beam and Optics Characterization,  
Québec, Canada, July 1996

F. Y. Génin<sup>a)</sup> and C. J. Stolz,

Lawrence Livermore National Laboratory,  
Laser Materials Department, Livermore, California 94550

### ABSTRACT

Hafnia-silica multilayer mirrors and polarizers were deposited by e-beam evaporation onto BK7 glass substrates. The mirrors and polarizers were coated for operation at a wavelength of 1053 nm at 45° and at Brewster's angle (56°), respectively. They were tested with a single 3-ns laser pulse. The morphology of the laser-induced damage was characterized by optical and scanning electron microscopy. Four distinct damage morphologies were found: pits, flat bottom pits, scalds, and delaminates. The pits and flat bottom pits (< 30 µm in diameter) were detected at lower fluences (as low as 5 J/cm<sup>2</sup>). The pits seemed to result from ejection of nodular defects by causing local enhancement of the electric field. Scalds and delaminates could be observed at higher fluences (above 13 J/cm<sup>2</sup>) and seemed to result from the formation of plasmas on the surface. These damage types often originated at pits and were typically less than 300 µm in diameter; their size increased almost linearly with fluence. Finally, the effects of the damage on the characteristics of the beam (reflectivity degradation and phase modulations) were measured.

**Keywords:** laser damage, morphology, HfO<sub>2</sub> SiO<sub>2</sub> multilayer, 1064 nm, mirror, polarizer

### 1. INTRODUCTION

Optical coatings are performance limiting components in high energy fusion laser systems such as the National Ignition Facility (NIF) at Lawrence Livermore National Laboratory (LLNL) or the Laser Mega-Joule (LMJ) in France. These lasers require coated optics that do not degrade the characteristics of the beam during operation lifetime.

This article will focus on characterizing the damage morphologies found in hafnia silica multilayer mirrors and polarizers after a single 3-ns pulse at 1064 nm and its effect on the characteristics of the beam. Future articles<sup>1,2</sup> will present the results on the stability of these multilayers during repetitive illumination.

The functionality of an optic can be characterized by understanding how damage initiates, how it grows during repetitive illumination and under environmental stress, and how such damage affects the properties of the transmitted or reflected beam (i.e. phase or amplitude modulations, reflectivity degradation, etc.).

The importance of damage morphology studies has been widely recognized<sup>3-36</sup> and many researchers have attempted to understand the relationship between damage morphology, damage threshold, and a variety of parameters such as wavelength,<sup>4-6</sup> fluence,<sup>7</sup> film material (composition and properties),<sup>4,8-26</sup> optical design<sup>9,27</sup> and film thickness,<sup>28</sup> pulse length,<sup>4,5,7,29-31</sup> and laser pulse repetition rate.<sup>29,32</sup> Understanding these relationships may allow process optimization so as to let the coating evolve (e.g. stress changes as a result of aging) while preventing catastrophic failure. In the 4 to 20-ns regime, a few conclusions were drawn from the literature. Damage is primarily influenced by the composition of the film. As the

---

<sup>a)</sup> Electronic Mail: fgenin@llnl.gov

number of layers in the stack increases, the damage threshold tends to decrease and approach that of the weaker component threshold.<sup>8</sup> Improvements are sometimes observed when a mixture of two materials of similar damage sensitivity but opposite stress characteristics (i.e.  $\text{SiO}_2$  and  $\text{MgF}_2$ ) have been prepared.<sup>33</sup> Permanent damage has always been recorded when a breakdown plasma is ignited. Finally, there is a general tendency for films with high scattering value and high optical absorption to damage more easily.

Several damage morphologies have been reported for high reflectors (HRs) irradiated at 1064 nm. Lowdermilk et al.<sup>34</sup> and Carniglia et al.<sup>35,36</sup> observed three morphology types in titania-silica and zirconia-silica HRs with silica overlayers: round and well defined damage sites 20 to 60  $\mu\text{m}$  in diameter, small pits 2 to 10  $\mu\text{m}$  in diameter, and large ill-defined spots 20 to 100  $\mu\text{m}$  in diameter. For non-overcoated HRs, they found an additional morphology corresponding to the removal of the coating over a large area (several hundred micrometers).

Pit formation as a result of inclusions has also been extensively studied both experimentally<sup>11,37-39</sup> and theoretically.<sup>40,41</sup> These studies have shown that nodular defect ejection depends on seed diameter and on incident laser fluence. This has provided some understanding in how laser damage and beam perturbations can be minimized through the process of laser conditioning.<sup>42</sup> The morphology of damage has also been found to depend on the wavelength, and pulse length. Walker et al.<sup>4</sup> reported that the damage morphology changes markedly with the laser wavelength. For example, at 0.26  $\mu\text{m}$ , oxide film materials damage in a uniform region while fluorides damage at isolated pits. This indicates that the precursors for damage and the damage mechanism can vary substantially with such parameters.

This article will only treat the case of hafnia-silica non-normal incidence mirrors and polarizers at 1064 nm tested with a 3-ns pulse. Only recently has hafnia been considered for such large scale coatings applications at LLNL and little was known so far about the damage morphologies for the hafnia-silica multilayer system. The morphologies were characterized using optical and scanning electron microscopy. Four distinct damage morphologies were identified: pits, flat bottom pits, scalds and delaminates. These morphologies which are shown in Figs. 1, 2, 3 and 4 will be discussed separately in the results section.

## 2. EXPERIMENTAL PROCEDURE

### 2.1 Mirror and polarizer coatings preparation

Both mirrors and polarizers were prepared by e-beam deposition of alternating layers of hafnia and silica onto BK7 Zygo polished substrates. The multilayers were coated at Optical Coatings Laboratory, Inc. (OCLI), Spectra Physics (S-P) and LLNL. Different sources and methods were used to deposit the film materials (e.g. hafnium oxide or metal hafnium in an oxygen partial pressure to deposit hafnia, etc.). Different sets of mirrors and polarizers were designed to operate respectively at 45° and 56° beam incidence. The mirrors were tested in both “S” and “P” polarization. The polarizers were tested in “S” polarization. The mirrors were overcoated with a half-wave silica overlayer. The polarizers were overcoated with a very thin silica layer only. A total number of 6 mirrors and 2 polarizers were tested. An average of 30 sites were irradiated on each sample. The sites were spaced 5 mm from one another to avoid conditioning effects from adjacent site illumination and minimize potential cross-contamination.

### 2.2 Laser testing conditions

The laser damage tests were carried out using a 3-ns pulse from a 1064 nm Nd:YAG laser. The laser was focused to provide a far field circular Gaussian beam with a diameter

of 1.1 mm at 86.6% of the maximum intensity. The beam profile was recorded for each shot and the peak fluence was computed. Each site was irradiated with a single laser pulse. The tests were conducted in “S” and “P” polarization at use angle. Two sets of mirrors were designed to reflect at  $45^\circ$  and  $56^\circ$ , respectively. The polarizers were designed to operate at  $56^\circ$ . Fluences during tests ranged from 5 to  $45 \text{ J/cm}^2$ . The sample was examined before and after irradiation by Nomarski and back light microscopy. Any damage larger than  $2 \mu\text{m}$  was detected. Further post damage characterization was conducted using scanning electron microscopy (SEM).

### 3. RESULTS

The results of the morphology study are first presented for the pits, flat bottom pits, scalds and delaminates. Table 1 summarizes the size information about the different morphologies. The effect of damage on the beam characteristics is then described.

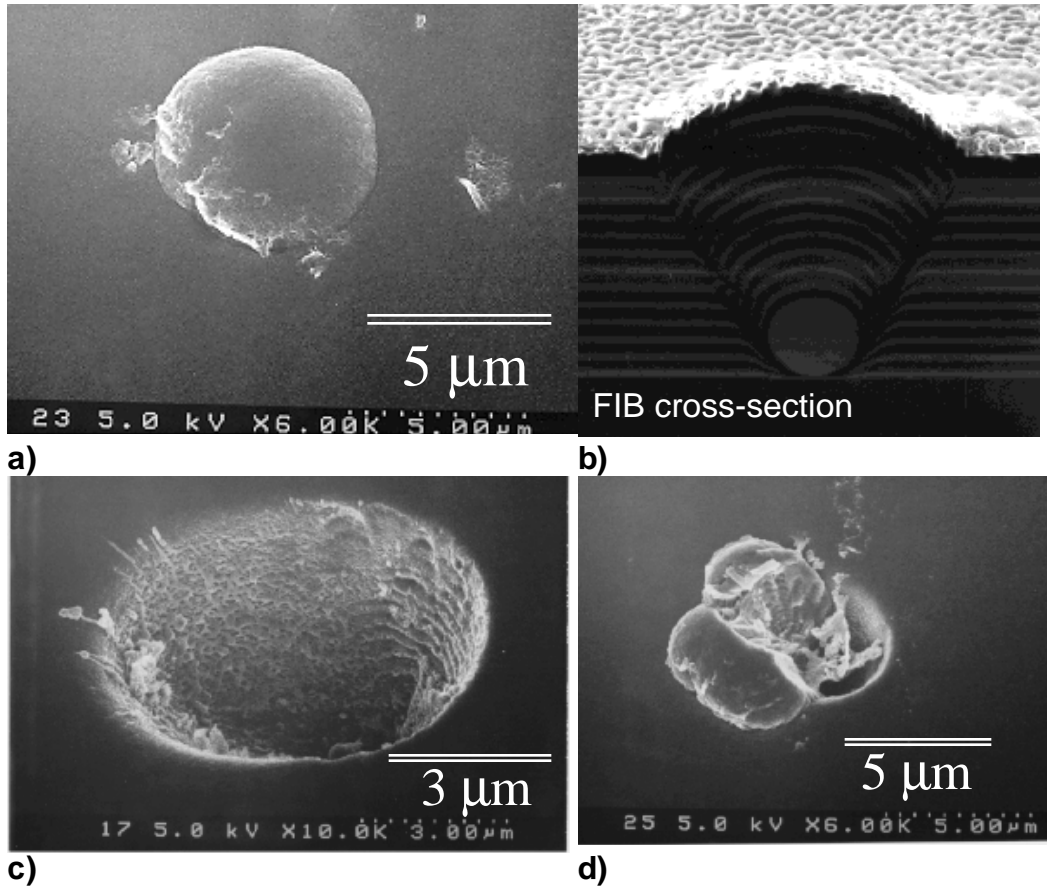


**Fig. 1:** SEM micrographs of a) a nodular defect in a multilayer mirror, b) a focused ion beam cross-section of a defect. The pit morphologies of the surface after nodular ejection is shown for c) shots at  $47.2 \text{ J/cm}^2$  at  $45^\circ$ , in “P” polarization and d) after a single shot at  $20.4 \text{ J/cm}^2$ . These micrographs illustrate cases where the nodules have been fully and partially ejected.

#### 3.1 Damage morphology

##### 3.1.1 Pits

It has been well established that pit formation results from the ejection of nodular defects in coatings.<sup>39</sup> Figs. 1.c) and 1.d) show the typical morphologies of nodules fully and partially ejected after laser illumination. The formation of pits can occur at very low fluence; such damage usually determines the conventional damage threshold of HRs and polarizers. At LLNL, the damage threshold is conventionally defined as the average between the lowest fluence which produces damage and the next lower fluence which does not produce damage. Such definition is simple but can have the disadvantage of not being representative of large area behavior since it can significantly depend on the number of sites tested. In general, the larger the tested area and the better the microscope resolution, the lower the measured damage threshold. When observed by back light optical microscopy with a 1  $\mu\text{m}$  detection limit, pinpoints can be observed when the site has been irradiated at 5  $\text{J}/\text{cm}^2$  and above. As shown in Fig. 5, the size of pits does not strongly depend on the fluence of the shot up to 40  $\text{J}/\text{cm}^2$ . Above 40  $\text{J}/\text{cm}^2$ , substantial collateral damage can occasionally occur. The plot shown in Fig. 5 is typical of the behavior of the mirrors. Similar plots were reported by Bliss et al.<sup>7</sup> for  $\text{TiO}_2\text{-SiO}_2$  and  $\text{ZrO}_2\text{-SiO}_2$  mirrors. The insensitivity of pit size on fluence at lower fluences can have a significant impact on how to improve the coatings' damage threshold by laser conditioning if no other damage morphologies are produced. From a functional stability perspective, no real benefit is added by conditioning if the pit morphology which determines the damage threshold does not grow with repetitive illumination and the total area of damage is insufficient to cause important losses of reflectivity. On the other hand, it is often difficult to produce coatings that satisfy this criterion.

### 3.1.2 Flat bottom pits

Flat bottom pits have been reported in a variety of multilayer systems<sup>36,43,44</sup> used at different wavelengths.<sup>45</sup> Similar morphologies have also been reported for single layers on glass substrates.<sup>43</sup> Fig. 2 shows a typical flat bottom pit morphology. Damage seems to propagate by delamination along the interface between two adjacent layers. Their cause is not yet fully understood and their formation does not always seem to correlate to defects detectable by optical microscopy. Like pits, the size of flat bottom pits does not strongly depend on the fluence of the shot below 35  $\text{J}/\text{cm}^2$  (see Fig. 5). A study by Walton et al.<sup>44</sup> has shown that the pit damage size depends on the overlayer thickness. Above 35  $\text{J}/\text{cm}^2$ , collateral damage is possible, in particular when pits are very large.

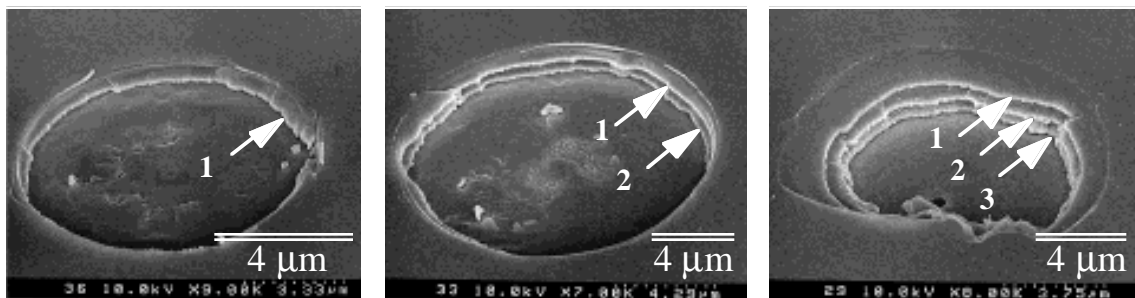


**Fig. 2:** SEM micrographs of various flat bottom pit morphologies after a single shot on a mirror at 15.2  $\text{J}/\text{cm}^2$  at 56°, in "P" polarization. The damage seems to propagate along the interface between silica and hafnia within the first three top layer pairs. Because of the contrast between the two oxides, hafnia appears lighter and silica darker.

### 3.1.3 Scalds

Scalds can be observed above 13  $\text{J}/\text{cm}^2$ . Fig. 3 shows a typical scald morphology. The scalds seem to be related to plasma formation. The surface of the coating appears to have "burnt". It is believed that electric field enhancements (e.g. at nodular defects or dust particles) can cause material and (or) air breakdown which produces a plasma. The plasma

expands during the shot and may lead to very high temperatures on the surface. The diameter of the scald increases almost linearly with the fluence (see Fig. 5). Other experiments<sup>46</sup> have also shown that their size increases with longer pulse lengths.

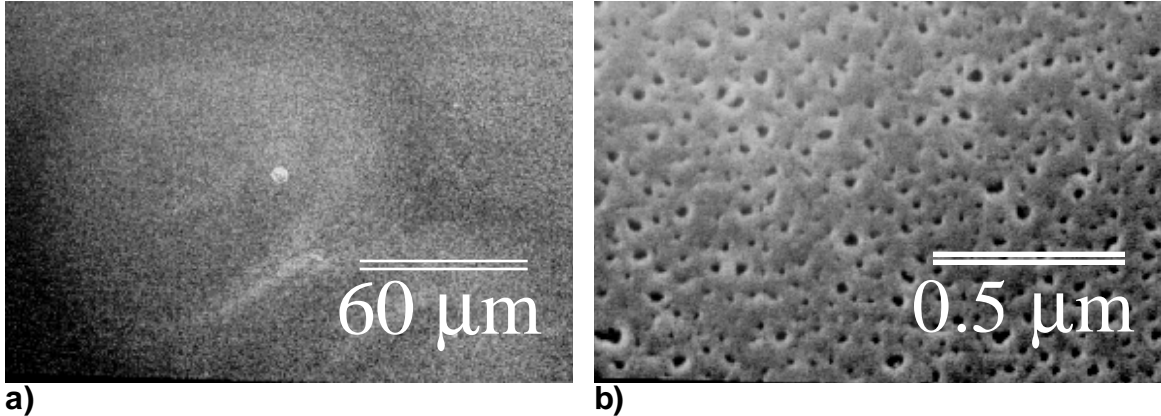


**Fig. 3:** SEM micrographs of a typical scald after a single shot at 45° on mirror irradiated at 41.6 J/cm<sup>2</sup> in “P” polarization. The micrograph on the left shows the details of the structure of the scald. The scald seems to have originated at a pit which is visible in the center of a).

### 3.1.4 Delaminates

Delaminates (i.e. removal of the overlayer) are very similar in size and shape to scalds. They are also found above 13 J/cm<sup>2</sup> when plasmas are observed to ignite and their size increases with higher fluences and longer pulse lengths (see Fig. 5). Like scalds, only the overlayer is damaged. However, while the silica overlayer remains attached to the coating for scalds, it is removed for delaminates. Fig. 4 shows a typical delaminate morphology. A pit is often found within the delaminated region. The failure mechanism is likely related to large gradients of temperature and stress in the top layers. Lowdermilk et al.<sup>34</sup> and other authors<sup>15</sup> have reported that the addition of a silica half-wave overcoat can substantially increase the damage threshold of HRs. A future article<sup>47</sup> will show that these findings also apply to polarizers and that the main factor contributing to such improvement is the prevention of delamination.

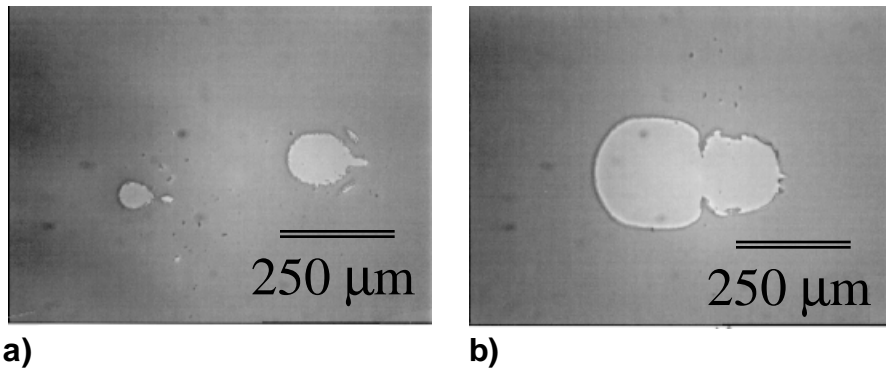


**Fig. 4:** Nomarski optical micrographs of delamination on the surface of a polarizer after a single shot at 56° in “S” polarization at a) 35.9 J/cm<sup>2</sup> and b) 38.7 J/cm<sup>2</sup>, respectively.

	pit	flat bottom pit	scald	delaminate
typical number of layers affected	between 2 and 50	2, 4, or 6	1	1
typical maximum diameter (μm)	20	30	300	400

**Table 1:** Typical number of affected layers and damage size of pits, flat bottom pits, scalds and delaminates after a single 3-ns laser pulse.

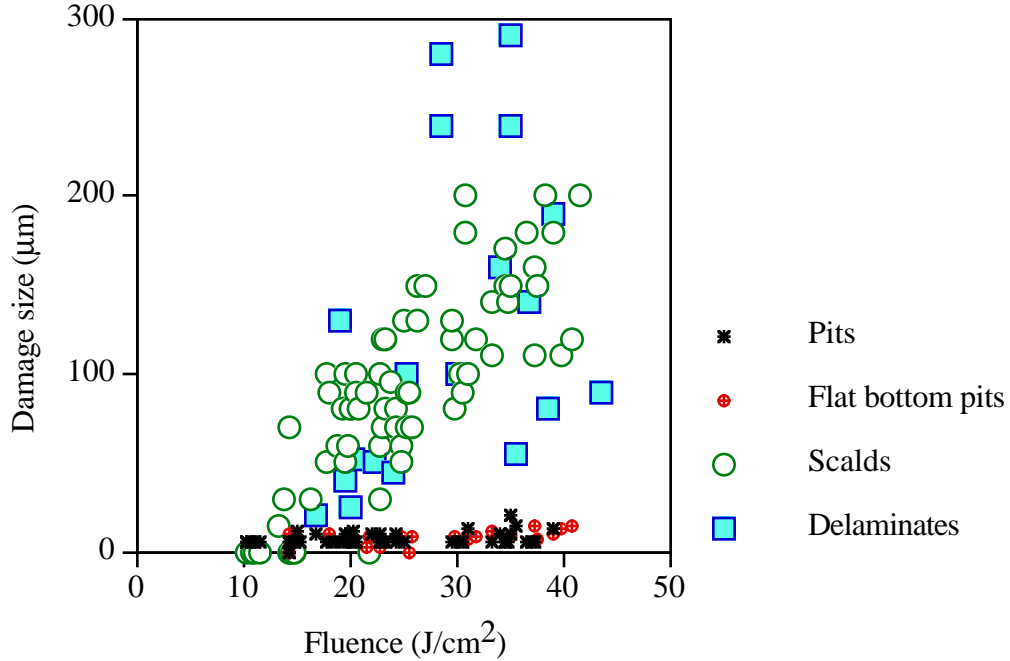


**Fig. 5:** Maximum damage size of the pit, flat bottom pit, scald, and delaminate morphologies as a function of fluence after a single shot. The measurements for the mirrors and polarizers of various origins (OCLI, S-P, LLNL) tested at 45 and 56° are plotted on this graph.

### 3.2 Effect of damage on the beam characteristics

When designing advanced fusion lasers, the effects of laser damage on beam propagation must be understood to maximize laser energy without putting additional downstream optics in the system at risk of laser-induced damage. Coated optical surfaces affect laser beams in a number of ways including transport efficiency due to the spectral, scatter, and obscuration characteristics of the coating and phase modulations resulting from diffraction and surface features. Laser damage in optical coatings enhances these effects.

#### 3.2.1 Transport efficiency

Mirror and polarizer coatings modify the reflective properties of a surface. The primary function of optical coatings in the NIF or LMJ are to direct laser beams from pulse generation to the target chamber with minimal energy loss.<sup>48</sup> Mirrors and polarizers are respectively required to reflect more than 99.5% at 1053 nm. Each of the four previously described damage morphologies interacts with the laser beam and reduces its overall energy. To achieve the laser system specifications, transport loss due to laser damage must be minimized and coatings need to be designed with a sufficient number of layers to compensate for minor reflectivity degradation.

The most obvious laser interaction involves scatter from a pit. Since the light is scattered in all directions, pits can be considered as obscurations. Bare optical surfaces for the NIF will be required to have a total obscuration less than  $10^{-5}$  of the total area of the optic. Obscurations from laser-induced pits can easily be treated in the same manner. Alternatively, if the entire optic meets the reflectance specification, the obscured area becomes irrelevant. Flat bottom pits and delaminates also scatter laser energy at the edge of the damaged region and hence behave similarly to pits.

The surface roughness of a coating is increased in a scald as seen in Fig. 3.b). It has been shown that surface roughness affects the scatter of incident radiation.<sup>49</sup> The increase in surface roughness results in an increase in scatter and reduction in reflection. Scalds can be observed under dark field optical microscopy; they therefore scatter more light than the background coating. To determine the influence of scalds on HRs, low spatial resolution reflectivity measurements were made of a large optic with numerous small scalds. A high spatial resolution scan of a large scald is shown in Fig. 5. The reflectivity of the coating is 99.8% and the standard deviation of the measurement is 0.12%. In both cases there was no detectable reduction in reflectance of the optic. Scalds will therefore not reduce the reflectivity below the 99.5% specification. Although the plasma scald in Fig. 5.b) does not degrade the coating below the reflectance requirements for a high reflector, the massive damage site in the center has a significant effect on the reflectance (about 75%) of the coating. This damage site was so large and unstable that the optic was removed from the laser system to prevent further damage to the coating and laser.

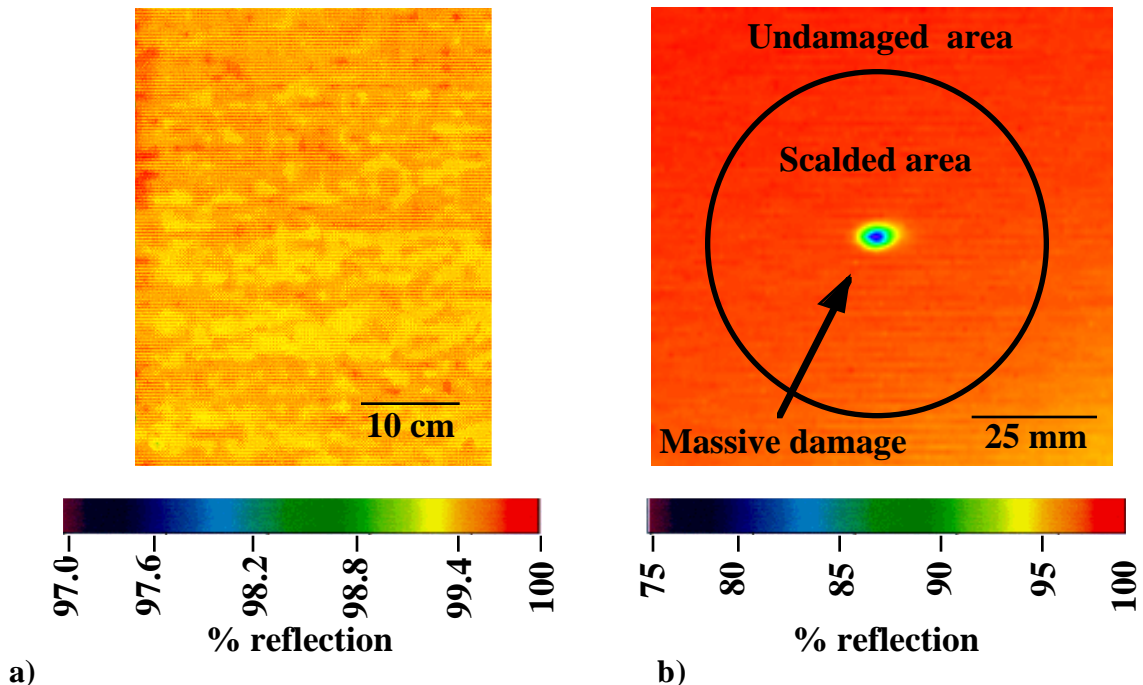


**Fig. 5:** Photometer scan of scalds a) low resolution reflectivity measurement of a laser conditioned mirror with numerous small scalds ( $<300\text{ }\mu\text{m}$  diameter)  $R_{\text{ave}} = 99.83\% \pm 0.12\%$ , b) high resolution reflectivity measurement of a single large (about 5 cm diameter) scald with no observable reflectance degradation in the scalded area.

### 3.2.2 Phase modulation

To understand changes to the coating's surface, scalds were measured using a Zygo GPI-XP phase modulating interferometer with a 33 mm beam compactor (see Fig. 7.a)). To estimate the effect of the scald damage morphology on beam propagation, a typical scald was modeled as a 200  $\mu\text{m}$  diameter micro-lens with a 6 nm sag. The diffraction limited spot size from an incident collimated beam with the same diameter as the scald is calculated from the relation  $2.44\lambda(f/\#) = 1\text{ cm}$  for  $\lambda = 1053\text{ nm}$ . The diffracted beam is significantly larger than the incoming beam and acts as a weak scatter site. In order for a 200  $\mu\text{m}$  plasma scald to focus light that could damage optics downstream, the sag must be larger than 270 nm ( $\lambda/4$ ) which is 45 times greater than what was observed for  $\text{SiO}_2$  overcoated multilayers.

Measurements by interferometry of pits and delaminates, as shown in Fig. 7.b), illustrate the difficulty of measuring a phase discontinuity or step function greater than half of the measuring wavelength. Possible methods to overcome this problem could include the use of dual or longer wavelength interferometers; they were not utilized in this study since the wavelength of interest was 1053 nm. To understand the impact of pits and delaminates on the beam, the damage sites were treated as circular obscurations as modeled by Hunt et al.<sup>50</sup> According to Hunt, the interaction of a wave scattered from an opaque obscuration with a background wave will produce holographic imaging, leading to increased fluences at image planes of the damaged optic. The magnitude of the intensity modulation is proportional to the size of the obscuration. Obscurations smaller than 280  $\mu\text{m}$  create intensity modulations that do not exceed the NIF specification, therefore become the upper bound for the maximum tolerable damage size. As mentioned earlier, future articles<sup>1,2</sup> will address the stability of damage under repetitive illumination. This will better define the maximum tolerable damage size of the NIF coated optics.

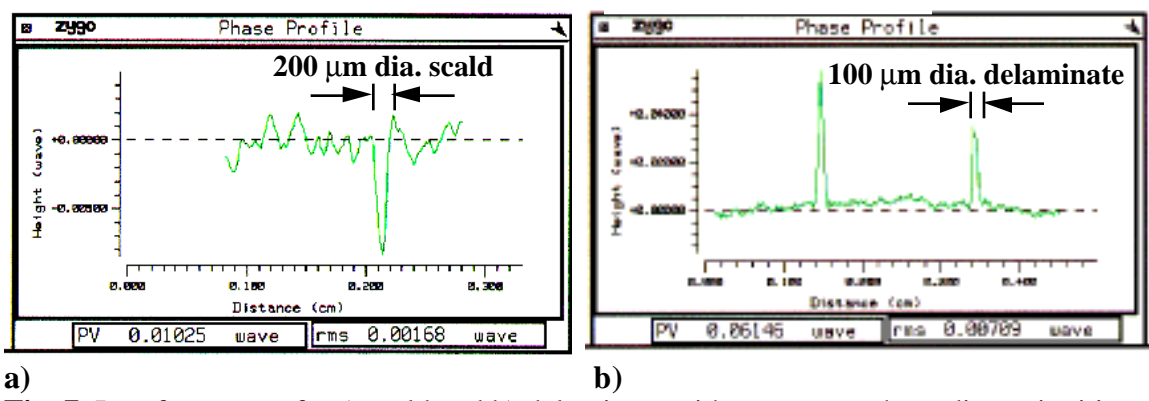


**Fig. 7:** Interferogram of a a) scald and b) delaminate with erroneous phase discontinuities.

#### 4. CONCLUSION

Hafnia silica multilayer mirror and polarizer coatings from various origins (OCLI, S-P, LLNL) were damaged during single shot laser tests at 1064 nm with a 3-ns pulse length at their respective use angle ( $45^\circ$  and  $56^\circ$ ). Four distinct damage morphologies were identified: pits, flat bottom pits, scalds and delaminates. The damage size was measured by Nomarski optical microscopy. The values reported provide the general trend of damage size as a function of fluence for the four damage morphologies.

The pits were found to be associated with the ejection of nodular defects. For the samples in this study, their diameter could reach 20  $\mu\text{m}$ ; they were observed at low fluences ( $5 \text{ J/cm}^2$ ) and could occasionally cause collateral damage at fluence above 40  $\text{J/cm}^2$ . The flat bottom pits were not very deep and usually involved only a few layers. They were not always associated with defects detectable by Nomarski optical microscopy and the failure mechanism occurred by interfacial delamination. Their characteristics (threshold and average size) were similar to those of pits, although they were often slightly larger than pits at a given fluence.

Scalds and delaminates were similar in size and shape (several hundred micrometers). They often originated at local defects such as pits and formed when plasmas were observed. Their diameter increased almost linearly with fluence and they usually formed above a fluence of  $13 \text{ J/cm}^2$ . Both morphologies involved the top layer and their occurrence were strongly influenced by the thickness of the overlayer. While the silica film looked “burnt” for scalds, it was removed for delaminates which, like for pits and flat bottom pits, points out to a difference in failure mechanism.

The four damage morphologies all influence beam propagation by increasing the scattered radiation which reduces the overall transport efficiency of the optic and creates beam intensity modulations. Since the scatter loss is not very significant compared to the total acceptable combined scatter and transmission loss of <0.5% for mirror and polarizer coatings, increasing reflection by optimizing the number of layer pairs in the coating design can compensate for the scattering loss. Scattered light that creates beam intensity modulations can be minimized by restraining the size of the damage. These results indicate that although no laser damage is desirable, some amount of damage can be tolerated and does not always interfere with the operation objectives of the laser system.

## 5. ACKNOWLEDGMENTS

This work was performed under the auspices of the U.S. Department of Energy by Lawrence Livermore National Laboratory under Contract W-7405-Eng-48. The authors wish to acknowledge Jim Yoshiyama for carrying out the SEM characterization of the films. Finally, many thanks are expressed to Ed Enemark (OCLI), Marc vonGunten (S-P) and Ron Bevis (S-P) for producing coatings for this study and to Sheldon Schwartz, Jean Hue and Mark Kozlowski for their valuable comments.

## 6. REFERENCES

1. F. Y. Génin, C. J. Stolz, and M. R. Kozlowski, submitted to the 1996 Boulder Damage Symposium.
2. F. Y. Génin, C. J. Stolz, M. R. Kozlowski, J. Atherton, and J. Hue, submitted to the 2nd Ann. International Conf. on Solid-State Lasers for Application to ICF (1996).
3. A. J. Glass and A. H. Guenther, *Appl. Optics* **12**, 637 (1973).
4. T. W. Walker, A. H. Guenther, C. G. Fry, and P. Nielson, *NBS SP* **568**, 405 (1979).
5. S. S. Wiseall and D. C. Emmony, *NBS SP* **669**, 102 (1982).
6. G. Pfeifer, E. Erben, G. Reisse, and B. Steiger, *SPIE* **2428**, 333 (1994).
7. E. S. Bliss, D. Milam, and R. A. Bradbury, *Appl. Optics* **12**, 677 (1973).
8. A. F. Turner, *NBS SP* **356**, 119 (1971).
9. R. R. Austin and A. H. Guenther, *NBS SP* **356**, 137 (1971).
10. R. R. Austin, R. Michaud, A. H. Guenther, and J. Putman, *Appl. Optics* **12**, 665 (1973).
11. D. Milam, R. A. Bradbury, and M. Bass, *Appl. Physics Letters* **23**, 654 (1973).
12. D. Milam, R. A. Bradbury, and M. Bass, *NBS SP* **387**, 124 (1973).
13. S. Holmes and P. Kraatz, *NBS SP* **387**, 138 (1973).
14. C. D. Marrs, W. N. Faith, J. H. Dancy, and J. O. Porteus, *NBS SP* **638**, 87 (1981).
15. T. T. Hart, T. L. Lichtenstein, C. K. Carniglia, and F. Rainer, *NBS SP* **638**, 344 (1981).
16. S. R. Foltyn and L. J. Jolin, *NBS SP* **688**, 493 (1983).
17. R. M. Wood, P. Waite, and S. K. Sharma, *NBS SP* **688**, 174 (1983).
18. N. S. Nogar, R. C. Estler, *NIST SP* **756**, 187 (1987).
19. E. Welsch, H. G. Walther, D. Schäfer, R. Wolf, and H. Müller, *Thin Solid Films* **156**, 1 (1988).
20. S. M. J. Akhtar, D. Ristau, J. Ebert, and H. Welling, *Phys. Stat. Sol. A* **115**, 119 (1989).
21. A. A. Tesar, *SPIE* **1441**, 228 (1990).

22. A. Chmel, A. Kondyrev, N. Leksovskaya, A. Radyushin, and Y. Shestakov, *Mat. Letters* **14**, 94 (1992).

23. L. J. Shaw-Klein, S. J. Burns, S. D. Jacobs, *Appl. Optics* **32**, 3925 (1993).

24. N. J. Hess, G. J. Exarhos, and M. J. Iedema, *SPIE* **1848**, 243 (1993).

25. S. Papernov and A. W. Schmid, *SPIE* **2428**, 333 (1994).

26. D. M. Spriggs, P. A. Sermon, M. S. W. Vong, and Y. Sun, *SPIE* **2714**, 537 (1995).

27. J. H. Apfel, E. A. Enemark, D. Milam, W. L. Smith, and M. J. Weber, *NBS SP* **509**, 255 (1977).

28. B. E Newnam, D. H. Gill, and G. Faulkner, *NBS SP* **435**, 254 (1975).

29. C. R. Giuliano and D. Y. Tseng, *NBS SP* **387**, 239 (1973).

30. K. Mann, H. Gerhardt, G. Pfeifer, B. Steiger, and F. Wenzel, *SPIE* **1624**, 319 (1992).

31. S. V. Garnov, S. M. Klimentov, A. A. Said, and M. J. Soileau, *SPIE* **1848**, 162 (1992).

32. R. M. Wood, P. Waite, and S. K. Sharma, *NBS SP* **669**, 44 (1982).

33. N. L. Boling, G. Dubé, M. D. Crisp, *Appl. Physics Letters* **21**, 487 (1972).

34. W. H. Lowdermilk, D. Milam, and F. Rainer, *NBS SP* **568**, 391 (1979).

35. C. K. Carniglia, J. H. Apfel, G. B. Carrier, and D. Milam, *NBS SP* **541**, 218 (1978).

36. C. K. Carniglia, J. H. Apfel, T. H. Allen, T. A. Tuttle, W. H. Lowdermilk, D. Milam, and F. Rainer, *NBS SP* **568**, 377 (1979).

37. T. A. Wiggins, and R. S. Reid, *Appl. Optics* **21**, 1675 (1982).

38. M. C. Staggs, M. Balooch, M. R. Kozlowski, and W. J. Siekhaus, *SPIE* **1624**, 375 (1991).

39. R. Tench, R. Chow, and M. R. Kozlowski, *J. Vac. Sci. Technol.* **A12**, 2808 (1994).

40. J. F. DeFord and M. R. Kozlowski, *SPIE* **1848**, 455 (1992).

41. R. H. Sawicki, C. C. Shang, and T. L. Swatloski, *SPIE* **2428**, 333 (1994).

42. L. Sheehan, M. Kozlowski, C. Stoltz, F. Génin, M. Runkel, S. Schwartz, and J. Hue, *Int. Symp. on Optical Systems Design and Production II*, Glasgow, U.K. (1996).

43. J. Dijon, J. Hue, A. Disgecmez, E. Quesnel, and B. Rolland, *SPIE* **2714**, 417 (1995).

44. C. Walton, F. Y. Génin, R. Chow, M. R. Kozlowski, G. E. Loomis, and E. Pierce, *SPIE* **2714**, 550 (1995).

45. A. Bodemann, M. Reichling, N. Kaiser, and E. Welsch, *SPIE* **2114**, 405 (1993).

46. J. Hue, F. Y. Génin, and S. Maricle, "Comparison of the single pulse delaminate damage size for 3-ns and 10-ns pulses", LLNL report (6-12-96).

47. C. J. Stoltz, F. Y. Génin, M. R. Kozlowski, R. Bevis, M. vonGunten, and J. Hue, submitted to the 1996 Boulder Damage Symposium.

48. W. A. Bookless, ed., *Energy Technology Review*, National Technical Information Service, Springfield VA, 1994.

49. J. M. Bennet and L. Mattsson, "Introduction to surface roughness and scattering", Optical Society of America, Washington DC, 1989.

50. J. T. Hunt, K. R. Manes, and P. A. Renard, *Appl. Optics* **32**, 5973 (1993).

*Technical Information Department* • Lawrence Livermore National Laboratory  
University of California • Livermore, California 94551